| | |
|---|---|
| Title | Influence of fire and drainage on evapotranspiration in a degraded peat swamp forest in Central Kalimantan, Indonesia |
| Author(s) | Ohkubo, Shinjiro; Hirano, Takashi; Kusin, Kitso |
| Citation | Journal of hydrology, 603, 126906<br>https://doi.org/10.1016/j.jhydrol.2021.126906 |
| Issue Date | 2021-12 |
| Doc URL | http://hdl.handle.net/2115/90757 |
| Rights | © 2021. This manuscript version is made available under the CC-BY-NC-ND 4.0 license<br>http://creativecommons.org/licenses/by-nc-nd/4.0/ |
| Rights(URL) | http://creativecommons.org/licenses/by-nc-nd/4.0/ |
| Type | article (author version) |
| File Information | Journal of Hydrology_603_126906.pdf |

# Influence of fire and drainage on evapotranspiration in a degraded peat swamp forest in Central Kalimantan, Indonesia

Shinjiro Ohkubo[1*], Takashi Hirano[1], Kitso Kusin[2]

*corresponding author

Address: Kita 9, Nishi 9, Kita-ku, Sapporo, Hokkaido 060-8589, Japan

E-mail: sohkubo@env.agr.hokudai.ac.jp

[1]Research Faculty of Agriculture, Hokkaido University, Sapporo 060-8589, Japan,

[2]CIMTROP, University of Palangkaraya, Palangkaraya 73112, Indonesia

**Keywords:** Groundwater level; Eddy covariance technique; Net radiation; Precipitation; Vapor pressure deficit

## 1. Introduction

Tropical peat swamp forests (PSFs) are widely distributed in Southeast Asia, especially Indonesia, Malaysia, Brunei, and Thailand (Page et al., 2011). However, in the recent decades, land conversion of forests mainly for agricultural use has been expanding. Deforestation and drainage accompanied by land use change result in peat aridification, which increase the risk of fire. Within 15.7 Mha of peatland in Peninsular Malaysia, Sumatra and Borneo, PSF decreased from 11.9 Mha in 1990 to 4.6 Mha in 2015, whereas managed land cover area (industrial plantations and small holder areas) increased from 1.7 Mha in 1990 to 7.8 Mha in 2015 (Miettinen et al., 2016). Nonetheless, large fires occurred repeatedly in this region. In 2015, the worst fire of the last two decades spread over Indonesia. As a result, smoke-induced haze engulfed insular Southeast Asia for a few months (Huijnen *et al.*, 2016; Ismanto et al., 2019).

Evapotranspiration (ET) plays a significant role in energy exchange and the water cycle between the terrestrial ecosystem and the atmosphere. Especially in tropical forests, ET has a significant impact on regional and global climate since ET is high enough to mitigate global warming by evaporative cooling effect (Bonan, 2008).

There are several studies examine how environmental disturbances such as fire, drainage, and deforestation affect ET. For example, in the tropical Amazon forest, deforestation decreased ET due to reduced transpiration and rainfall interception and subsequent evaporation (Baker and Spracklen, 2018). In the other study from the Amazon forest, ET in logged or burned forest was generally smaller than that in the intact forest because of lower leaf index, whereas the difference became smaller under extremely dry conditions (Longo et al., 2020). In boreal peatland where feather moss dominated, ET increased or decreased depending on peat burn severity (Kettridge et al., 2017; Kettridge et al., 2019; Wilkinson et al., 2020). They explained that evaporation from peat soil surface increased as the capping layer of feather moss disappeared by a severe fire, whereas ET decreased by light burning which made soil surface became water-repellent and restrict the supply of water to the peat surface.

Other than peatland site, some studies observed reduction of ET after a fire, and cited loss of transpiration due to leaf burning as the reason (i.e., Beringer et al., 2003; Clark et al., 2012; Montes-Helu et al., 2009; Whelan et al., 2015). A decline in net radiation ($R_n$) is also cited as the reason for decreased ET. For example, Liu et al. (2005) explained that forest canopies cleared by fire increased ground temperature and upward longwave radiation, resulting in a decrease in $R_n$. Montes-Helu et al. (2009) explained that the exposure of the soil surface and the increase in bright-colored coarse woody debris (CWD) increased the albedo after a fire.

On the other hand, drainage significantly and directly impacts the water budget by increasing the underground outflow. Mezbahuddin et al. (2015) reported that drainage reduced ET due to drawdown of groundwater level (GWL) and soil drying using a process-based model that relied on field data from tropical PSFs. They explained that the reduced water uptake of shallow roots due to aridification cannot be compensated by the water uptake of deep roots. Alternately, Moore et al. (2013) found that ET was lowest at the driest site among three adjacent peatland sites. Especially in peatlands, desiccation of soils due to lowering of GWL create aerobic conditions and accelerate the decomposition of peat then increase the release of $CO_2$ into the atmosphere.

Although previous studies revealed the influence of such disturbances on ET, Hirano et al. (2015) is the only one of its kind with continuous field observation in tropical PSFs. They had been conducted observations for 4-6 years until 2009 in three tropical PSFs with different degrees of disturbances in Central Kalimantan, Indonesia. They revealed that almost intact forest had high annual ET comparing with those in other upland tropical forests. A significant difference in annual ET was not found between in almost intact and drained forests, although minimum-monthly-mean GWL had a positive linear relationship with the ET. The result suggested that tree species in drained forest acclimatized to a low GWL environment after more than 5 years after drainage. In burnt ex-forest, ET was decreased due to vegetation loss.

Nonetheless, the response of ET to change in environmental factors (e.g., $R_n$, VPD, GWL) in the vegetation regenerating process immediately after the fire is still unknown since the observation had started several years after the fire and drainage. And the response to precipitation ($P$), which is the only water-supplying element to the system, was not cleared under excessively GWL-lowered conditions.

We continued the observation in the ex-PSF site in Hirano et al. (2015) through 2016, with a brief suspension by fire in 2009. During the continued observation period, the study site experienced fires and drainage. In particular, the fire burned CWD mostly in 2009 then succeeding vegetation regenerated immediately in subsequent La Niña years (Ohkubo et al., 2021b). Thus, the site turned to be carbon sink from $CO_2$ source. These two disturbances are expected to have a lingering effect and to manifest at different time scales. In other words, vegetation regeneration is long-term while GWL fluctuations occur on a shorter time scale. Therefore, we need continuous and long-term observation for examining the effect of the disturbances. Moreover, the continuous long-term observation with a variety of environmental conditions enables us to reveal ET variation through fire and drainage disturbances and to examine characteristics of ET response to environmental changes with accumulated data.

Here, we have an unprecedented long-term dataset through fire and drainage events from 2004 to 2016. In this study, we estimated ET considering the contribution to energy and water balance and explored the significant controlling factors of ET through the fire and drainage disturbances. Then, the data was also used to answer the following specific questions: (i) how changes in ET were influenced by meteorological factors in the process of vegetation recovery from fire, and (ii) how do the sensitivity of ET to *P* and GWL change after canal excavation.

## 2. Materials and Methods

### 2.1 Site description

The study site (2.34 ° S, 114.04 ° E) is located in tropical peatlands near Palangkaraya City, Central Kalimantan, Indonesia (Fig. 1). The site was called DB - a drained burned degraded PSF in our previous study (Hirano et al., 2015). The site was a tropical degraded PSF until the fire in 1997. Since then, the site had been burned at least three times in 2002, 2009, and 2014. The mean annual temperature and *P* measured at 1.5 m height from 2005–2016 were 26.4 ± 0.3 °C and 2640 ± 473 mm (mean ± 1 standard deviation), respectively. The site experienced the dry season (monthly $P < 100$ mm), usually from July to October. During the observation period from April 2004 to

December 2016, the study site experienced fires and canal excavation. In 2009, the study site experienced moderate fire, and some aboveground herbaceous plants were burned. In 2014, a less severe fire burned the study site again. In 2015, the surrounding area experienced fire, although the study site was not affected. More detailed information is described in Ohkubo et al. (2021b). In May–June 2014, a canal was constructed in the vicinity of the site. To analyze the influence of the disturbances and environmental changes, we divided the observation into three periods: Period I (May 2004–September 2009), Period II (December 2009–June 2014), and Period III (July 2014–October 2016) (Table 1). During Period I, CWD was present on the ground and vegetation was slowly regenerating since the fire in 2002. Initially (April 2004), fern (*Stenochlaena*, *Blechnum,* and *Lygodium* spp.) and sedge (*Cyperus*, *Scleria,* and *Eleocharis* spp.) plants were sparsely distributed. In June 2005, peat soil was mostly covered with 0.5 m high fern and sedge plants. A few young trees, comprised predominantly of *Combretocarpus rotundatus,* reached a height of 0.8–0.9 m before the fire in 2009. In September 2009, some of the trees died and a part of the above ground herbaceous plants were burned by fire of moderate-severity. A large amount of CWD was also burned out. During Period II, ferns and sedges covered the ground surface immediately after the fire of 2009. Sparsely distributed young trees, predominantly

*Combretocarpus rotundatus*, grew up to 2-m high until 2013. Woody plants dominated the latter phase of Period II. A water-logged condition lasted a long time following abundant $P$ during La Niña years (2010–2011). A small canal about 1.5-m deep and 1.5-m wide was excavated approximately 100 m away from the observation tower from May–June 2014. In September 2014, the study site was burned again by fire of low-severity. Herbaceous plants and some young trees were burned, whereas many trees survived. In 2015, fire occurred in the surrounding area, but the study site was not affected. Hence, during El Niño drought in 2014 and 2015, the site experienced severe haze caused by the fires. Further information is described in earlier studies (Hirano et al., 2014; Hirano et al., 2015; Itoh et al., 2017), and our accompanying papers on albedo (Ohkubo et al., 2021a) and $CO_2$ flux (Ohkubo et al., 2021b).

## 2.2 Measurements

Observations were conducted from April 2004 to December 2016. Air temperature and relative humidity at a height of 1.5 m were measured with a platinum resistance thermometer and a capacitive hygrometer (HMP45; Vaisala, Helsinki, Finland) installed in a non-ventilated radiation shield (DTR503A; Vaisala). $P$ was measured with a tipping-bucket rain gauge (TE525; Campbell Scientific Inc.) at a height of 1.5 m. $R_n$

was measured with a radiometer (CNR-1; Kipp & Zonen, Delft, the Netherlands). The measurement height was raised following tree growth; height of 3.3 m (April 2004–May 2012), 6.8 m (May 2012–December 2013), and 13.6 m (December 2013–December 2016). Their 30-min averages were recorded using data loggers (CR1000 and CR10X; Campbell Scientific Inc.). GWL was measured with a water level logger (DL/N; Sensor Technik Sirnach AG, Sirnach, Switzerland or DCX-22 VG; Keller AG, Winterthur, Switzerland) at an interval of every 30 min. GWL is the relative groundwater level from the ground surface, and negative GWL means that water surface is below the ground surface. Reference ground surface level was corrected since significant subsidence was observed after fire in 2009. The soil heat flux ($G$) was not measured, and vapor pressure deficit (VPD) was calculated from acquired air temperature and relative humidity data. Eddy fluxes of sensible ($H$) and latent heat ($\lambda E$) were measured with a sonic anemometer-thermometer (CSAT3; Campbell Scientific Inc., Logan, UT, USA) and an open-path $CO_2$/$H_2O$ analyzer (LI7500; Li-Cor Inc., Lincoln Nebraska, USA) using the eddy covariance technique. The measurement height was raised: height of 3.0 m (April 2004 to February 2011), 3.6 m (February 2011–March 2012), 7.2 m (March 2012–December 2013), and 13.6 m (December 2013–December 2016). The two sensors were separated by 0.2 m.

The monthly ΔGWL was calculated from the difference between the mean of GWLs taken at half-hourly intervals of the last days of two adjacent months. The observation system was suspended from September 20 to December 4, 2009, as the power cables and sensors were severely damaged by fire. Eddy flux data of $H$ and $\lambda E$ were available up to November 5 and October 27, 2016, respectively, due to sensor malfunction. Further information about instruments and data collection is described in Hirano et al. (2015) and our accompanying paper on $CO_2$ flux (Ohkubo et al., 2021b).

## 2.3 External data

The enhanced vegetation index (EVI) in MODIS data (MOD13Q1 Version) was downloaded from the "Land Processes Distributed Active Archive Center" (https://lpdaac.usgs.gov/products/mod13q1v006/). The data were composited every 16 days at a spatial resolution of 250 m. Monthly Southern Oscillation Index (SOI) data were collected from "National Oceanic and Atmospheric Administration" (https://www.ncdc.noaa.gov/teleconnections/enso/indicators/soi/). SOI which is a standardized index based on the observed sea level pressure differences between Tahiti and Darwin, Australia, is an indicator of El Niño and La Niña episodes. In general, prolonged periods of negative (or positive) SOI values coincide with El Niño (or La

Niña) episodes.

## 2.4 Flux calculation

$H$ and $\lambda E$ were calculated using Flux Calculator software (Ueyama et al., 2012) with the following procedures: (i) removal of spikes (Vickers and Mahrt, 1997), (ii) double rotation for tilt correction, (iii) water vapor correction for virtual temperature, (iv) correction for high frequency loss (Massman, 2000; Massman, 2001), and (v) correction for air density fluctuations (Webb et al., 1980). Data with wind directions within ±20 ° from the north were excluded to avoid flow distortion by the tower. Data were also removed when precipitation was detected. Data with $H \leq -200$, $H>500$, $\lambda E \leq -100$, and $\lambda E >1000$ W m$^{-2}$ were screened as outliers. A stationarity check was performed for each 30-min run (Foken and Wichura, 1996), and we calculated the difference between covariance values for the entire 30 min and the average of six 5-min covariance values. Data were excluded, in case the difference was more than 100%. To investigate the development of the turbulence, integral turbulence characteristics (ITC) was calculated every 30 min (Foken, 2017), then $H$ and $\lambda E$ with ITC>250% was excluded after stationarity check. After these data quality controls, monthly data with high gap fractions (e.g., more than 70% of half hourly data are missing) was removed from the analysis. However, they are used to illustrate monthly variations and estimate annual values.

Gaps in $H$ and $\lambda E$ data were filled using the lookup table method. Look-up tables for each $H$ and $\lambda E$ were created for every three months considering climate conditions as the previous study applied (Hirano et al., 2015), i.e., February–April, May–July, August–October, November–January, using half-hourly $R_n$ and VPD. First, the data were binned equally into ten classes according to $R_n$. Second, the classified data in each class were binned equally into three classes according to VPD. Finally, values in 30 classes were determined by averaging each binned data. Look-up tables of $H$ and $\lambda E$ from August to October 2016 were substituted for those of November–December 2016, respectively, due to the lack of eddy flux data. The mean half hourly $(H+\lambda E)/R_n$ was 0.74 ± 0.06 (mean ± 1 standard deviation) on an annual basis (Table S1). To settle the energy imbalance, after filling the gaps, $H+\lambda E$ was forced to balance with $R_n$ on a daily basis, maintaining a constant ratio of cumulative daily $H$ and $\lambda E$ at this study site (Twine et al., 2000). We used this adjusted $\lambda E$ for calculating ET in this study. Detailed procedures are described by Hirano et al. (2015).

## 2.5 Bulk parameters

Physiological regulation of vegetation canopy (i.e., integrating stomatal regulation of individual leaf) or surface wetness for ET could be expressed by surface conductance ($G_s$). Decoupling between vegetation and the atmosphere for ET was evaluated by index $\Omega$, where ET is controlled by stomatal regulation when $\Omega \approx 0$ and by available energy when $\Omega \approx 1$. We used $H+\lambda E$ instead of $R_n-G$ because $G$ was not measured. Then, the bulk parameters of $G_s$ and $\Omega$ were calculated following the method of Hirano et al. (2015) as:

$$\frac{1}{G_s}=\frac{1}{G_a}\left[\frac{\varepsilon(H+\lambda E)+\rho C_p G_a \frac{VPD}{\gamma}}{\lambda E}-\varepsilon-1\right], \tag{1}$$

$$G_a=\left[\frac{2}{k u_*}\left(\frac{dh}{dv}\right)^{\frac{2}{3}}+\frac{u}{u_*^2}\right]^{-1} \tag{2}$$

$$\Omega=\frac{\varepsilon+1}{\varepsilon+1+\frac{G_a}{G_s}} \tag{3}$$

where $G_a$ is the bulk aerodynamic conductance (m s$^{-1}$), $\varepsilon$ is the slope of the relationship between saturated vapor pressure and temperature, $\rho$ is air density (kg m$^{-3}$), $C_p$ is the specific heat of air at constant pressure (=1007 Jkg$^{-1}$ K$^{-1}$), $\gamma$ is the psychrometric constant (=0.067 kPa K$^{-1}$), $k$ is the von Karman constant (=0.4), $u_*$ is the friction velocity (m s$^{-1}$), $dh/dv$ is the ratio of thermal diffusivity to molecular diffusivity of water vapor, and $u$ is the wind speed (m s$^{-1}$). To avoid instability and divergence, we used midday ecosystem conductance (1000–1400 h) without rain data to calculate mean monthly values.

## 2.6 Path analysis

We conducted path analysis to explore the main controlling factors of monthly ET using the R package *sem* version 3.1-11. $P$, $R_n$, VPD, GWL, and EVI were selected as explanatory variables. Each path coefficient, i.e., the direct effect of each explanatory variable was standardized. The total effect was determined by the sum of the direct and indirect effects. The model structure was adjusted as goodness-of-fit index (GFI) improved. Sun et al. (2018) described the criteria that the GFI of an adequate model is greater than 0.9.

# 3. Result

## 3.1 Overview of time-series variations

We compared ET with environmental factors and energy fluxes in a time series (Fig. 2). ET seemed to be stable regardless of $P$ fluctuation, although it decreased with deep GWL conditions (GWL < -0.5 m) (Fig. 2a, b). The mean annual ET was 1457 ± 152 mm (mean ± 1 standard deviation) (Table 2). Until the canal excavation from May–June 2014, GWL generally deepened in the dry season and increased and reached the ground surface level in the wet season. However, GWL never recovered to the ground surface level after canal excavation despite much $P$ in 2016. VPD showed seasonal variation with high values in the dry season. The monthly average VPD exceeded 10 hPa during the fires in 2004, 2009, 2014, and 2015 (Fig. 2c). $\lambda E$ and $R_n$ fluctuated in synchrony and had prominent troughs in 2004, 2006, 2014, and 2015 (Fig. 2d). In contrast, $H$ fluctuated slightly. The annual Bowen ratio ($\beta = H/\lambda E$) calculated from cumulative $H$ and $\lambda E$ for whole year, was 0.31 ± 0.07 (mean ± 1 standard deviation) but $\beta$ occasionally increased with fire. (Fig. 2e, Table 2). Maximum $\beta$ (0.74) was recorded in October 2014. $G_s$ decreased with increased VPD in the dry season (Fig. 2f). $\Omega$ had constant high values of approximately 0.8 under water-logged conditions (2010–2013) and decreased with increasing VPD (Fig. 2f). EVI decreased with fire in 2009, 2014, and 2015, and subsequently increased gradually after every fire (Fig. 2g). Negative values of SOI were seen in El Niño years (2004–2005, 2006–2007, 2009–2010 and 2014–2016) whereas the positive values were seen in La Niña years (2005-2006, 2007-2008, 2008-2009, 2010–2012 and 2016) (Fig. 2h). Especially, SOI had been positive for a long period during 2010–2012 and there was much of $P$. During or after fires, a decrease in ET was observed in 2004, 2006, 2014, and 2015 with temporarily lowered $R_n$ very likely due to fire-induced haze. Immediately after drainage, ET did not decrease but decreased thereafter when GWL was extremely deep.

Comparing the mean monthly ET in the three periods (Table 3), ET was the largest with 136 mm month$^{-1}$ in Period II followed by 119 mm month$^{-1}$ in Period I and 109 mm month$^{-1}$ in Period III. As for the comparison of meteorological conditions, the largest $P$ (253 mm month$^{-1}$) and $R_n$ (407 MJ m$^{-2}$ month$^{-1}$), and lowest VPD (6.27 hPa) were observed in Period II. In Period III, GWL was deepest (- 0.50 m), although $P$ was similar to that in Period I. Smallest $\beta$ (0.23), and largest $G_s$ (10.76 mm s$^{-1}$) and $\Omega$ (0.69) were recorded in Period II.

## 3.2 Water and energy balance

In terms of water balance, $P$ is a unique factor that supplies water to the ombrotrophic peatland. We examined the relationship between ET and $P$ on a monthly basis (Fig. 3), and a positive correlation ($R = 0.38$, $p < 0.01$) was found for the whole observation period. However, when $P$ was greater than ET, ET fluctuated around 127 ± 17 mm (mean ± 1 standard deviation) independently of $P$. Therefore, annual ET/$P$ became smaller as $P$ became larger. The mean annual ET/$P$ was 0.56 ± 0.07 (Table 2). In contrast, when $P$ was less than ET, ET decreased in some months when GWL< -0.5 m in Periods I and III, although, decreased ET (~ 50 mm month$^{-1}$) was observed for one month (October 2015) even when ET< $P$. On the contrary, there was no condition with

GWL< -0.5 m in Period II.

We examined the relationship between monthly changes in GWL (ΔGWL) and precipitation surplus ($P$−ET) (Fig. 4). We exclude the data with GWL $\geq$ -0.1 m to exclude the case of surface outflow, which could not be evaluated quantitatively in this study. Significant positive correlations between $P$−ET and ΔGWL were observed for all periods. Significant difference ($p<0.01$) was not found between the fitted lines in Periods I and II. X-axis intercepts of the fitted lines were -6.3, 1.0, and 117.4 mm in Periods I, II, and III, respectively. The underground outflow specifically increased in Period III. Additionally, the slopes of the fitted lines were $3.60\times10^{-3}$, $2.74\times10^{-3}$ and $1.30\times10^{-3}$ m mm$^{-1}$ in Period I, II and III, respectively.

We examined the relationship between $\beta$ and $R_n$, and $\beta$ and VPD in case of $R_n \geq 600$, respectively (Fig. 5). As $R_n$ increased, $\beta$ became larger and the increasing rate became gentle in all periods. In period II, $R_n$-filtered ($R_n \geq 600$) $\beta$ had a decreasing trend with VPD contrary to the increasing trend which were seen in Period I and III.

## 3.3 Relationship between ET and environmental factors

Half-hourly ET had a strong positive correlation with $R_n$ throughout the observation period (R=0.89, $p<0.01$, Fig. 6a). VPD also had a positive correlation with ET when

VPD<20 hPa, and ET was stable irrespective of VPD when VPD≥20 hPa (Fig. 6b). Quadratic curve of GWL was applied for each Period but positive correlation was seen when GWL<-0.5 m (Fig. 6c). No significant correlation was found between ET and EVI for each of the three periods as well as for the whole measurement period (-0.08−0.22 and 0.00, Fig. 6d). ET had positive relationship with $G_s$. The increasing trend of ET to $G_s$ became more gradual as $G_s$ increased (Fig. 6e). In Period II, $G_s$ fluctuated in the higher $G_s$ range, as compared with $G_s$ in Periods I and III. ET seems to be stable irrespective of $\Omega$ when $\Omega \geq 0.5$. When $\Omega < 0.5$, increasing trend of ET with $\Omega$ was seen in Period III whereas ET hardly fluctuated in Period I.

### 3.4 Path analysis

To analyze the contribution of each environmental factor, we drew a path diagram (Fig. 7a). $P$ had a positive (Fig. 7b) and $R_n$ had the largest effect (0.73–0.92) in all periods. VPD had negative effects in Period I (-0.64), III (-0.26), and whole period (-0.27), whereas the effect was negligible in Period II (0.05). GWL had a positive effect in Period I (0.35) and II (0.34), whereas the effect was negative in Period III (-0.09). EVI had a significant effect (0.18) only in Period III. The goodness-of-fit index (GFI) is 0.86–0.96. All path coefficients are listed in Table 4.

# 4. Discussions

## 4.1 Comparison of ET with other studies

The mean monthly ET (109–136 mm, Table 3) at the study site was larger than those observed in three boreal peatland sites (12–103 mm (Petrone et al., 2014; Sottocornola and Kiely, 2010; Wu et al., 2010). In other words, even though the mean ET decreased after drainage in Period III, it was still larger than the maximum ET recorded in the growing season at the boreal peatland site. In contrast, ET/*P* (0.56) in the study site (Table 2) was smaller than those in boreal peatland sites (ET/*P*=0.90 (Brust et al., 2018), ET/*P*=0.79, (Fraster et al., 2001), and ET/*P*=1.07 (Morison et al., 2020)). On the other hand, annual ET and ET/P (1222–1662 mm and 0.44–0.66, Table 2) in this study site were generally similar to those in Borneo's forest (1210–1545 mm and 0.46–0.72, Kumagai et al., 2005; Kume et al., 2011). A small ET/*P* would be characterized by a large amount of *P* in this tropical regions, although ET was somewhat larger than those in boreal peatland sites. Compared with $\lambda E$ in other tropical sites reported by Fisher et al. (2009), $\lambda E$ in our study was generally smaller than $\lambda E$ in rainforests in America ranged 1.72°S–10.42°N, and was similar to $\lambda E$ in plantations in Congo and Vanuatu and pastures in America which ranged 3.01°S–15.44°S. Similar $\lambda E$ would be because have nearly identical above-ground biomass. Being different from the result of comparison in ET, $\lambda E$ in this study was smaller than $\lambda E$ in other tropical forest. Nevertheless, the difference of $\lambda E$ will be closer if $\lambda E$ in our study is corrected so that the energy balance ($R_n - G = H + \lambda E$) is closed. Wet condition with sufficient $P$ would increase evaporation thus ET, even when peatlands experienced terrestrial disturbances. Compared with ET/$P$ in Period I, the smaller ET/$P$ in Period II could be explained by significantly increased $P$ due to a La Niña event, although ET increased somewhat (Table 3). Alternately, smaller ET/$P$ in Period III could be explained by smaller ET because $P$ in Period III was similar to that in Period I. As shown in Fig. 4, drainage increased underground outflow, i.e., available rainwater for ET would be reduced in Period III.

Compared with mean ET in undrained (136 mm month$^{-1}$, 2004–2008) and drained (129 mm month$^{-1}$, 2002–2008) PSFs in the vicinity of the study site (Hirano et al., 2015), ET in Period II was similar to the above values, whereas ET in other periods was smaller. Specifically, with waterlogged conditions during La Niña years, ET was comparable to those in forest sites under normal meteorological conditions, even though some above-ground vegetation was burned. These results indicated that continuous rainfall which brings waterlogged condition has potential to increase ET in tropical peatlands.

### 4.2 Low $\beta$ with recovered vegetation and wet condition after fire

Mean annual $\beta$ (0.22–0.39) was smaller than tropical savanna (1.4–7.0, Beringer et al., 2003), boreal peatland (1.10–1.19, Morison et al., 2020), upland forest of North America (0.5–1.0, Moore et al., 2013) and arctic wetlands at several sites (0.56 on average, Lafleur, 2008), and similar to the average in tropical ecosystems which mostly comprise of forests (0.3, Fisher et al., 2009)). This indicates that a large part of $R_n$ was distributed to $\lambda E$ irrespective of fire and drainage disturbances at this tropical site, although there was some residual energy ($R_n - H - \lambda E$). Contrary to the results of earlier studies (e.g., Beringer et al., 2003; Morison et al., 2020; Whelan et al., 2015), fire decreased $\beta$ in Period II. Earlier studies described that $\beta$ increased with decrease in ET due to loss of vegetation. D'Acuncha et al. (2018) reported that fire decreased ET from 4.5 to 2.5 mm day$^{-1}$ by burning species of trees. In the study site, vegetation recovered immediately in post-fire years due to large $P$ with La Niña events. This could be one reason for the small $\beta$ with recovered ET after fire at this site. Under conditions where the effect of $R_n$ on $\beta$ was small, decreasing $\beta$ with VPD was found in Period II whereas the increasing trend was found in Period I and III (Fig. 5b). As mentioned in the previous subsection, waterlogged condition lasted for a long period with prolong rain after fire in Period II (Fig. 2b). Always wet condition which increases evaporation could be another reason for the small $\beta$, although decrease in $\beta$ does not necessarily mean increase in ET. Thus, our result showed the case that subsequent meteorological condition somewhat counteracts the effect of fire on $\beta$, although fire potentially increase $\beta$ due to loss of transpiration.

### 4.3 Strong dependence of ET on $R_n$ through the fire and drainage

$R_n$ had a significantly high positive correlation with ET ($R = 0.89$, $p<0.01$, Fig. 6a) and the largest effect on ET throughout the observation period (0.73–0.92, Fig. 7b). A strong correlation was found in other studies (Morison et al., 2020; Wang et al., 2020). This indicates that fire and drainage disturbances did not change the characteristics of strong dependence on $R_n$. And fire could indirectly decrease ET by generating haze which attenuate incoming radiation. On the other hand, $\Omega$ became larger ($\Omega=0.69$) with shorter vegetation of ferns and sedges in Period II and became smaller ($\Omega=0.56$) with emerging woody plants in Period III (Table 3). These results explained that stomatal regulation became significant for ET via change of transpiration rate as canopy layer became thicker. On the other hand, atmospheric conditions (e.g., $R_n$, VPD) control ET rather than stomatal behavior in short vegetation since incoming solar radiation is likely to reach the ground surface and evaporation contributes to ET more. The variation of $\Omega$ coincide with those of previous studies. Jarvis and McNaughton (1986) reported that $\Omega$ is larger with shorter vegetation and vice versa: grassland 0.8, wheat 0.6, and forest 0.2. $\Omega$ of regenerating forest decreased from that of the bog in Central Siberia (Valentini et al., 2000). Fire would increase the dependence on $R_n$ by clearing vegetation.

### 4.4 Vegetation succession post fire controls ET sensitivity to EVI

A significant correlation between EVI and ET was not seen in this study (Fig. 6d), whereas previous studies found a positive correlation between vegetation indices and ET. For example, Wang et al. (2020) reported that ET increased with land conversion from bog to pasture. They estimated an increase of $\lambda E$ with 54 $\mathrm{Wm^{-2}}$ for a unit difference of EVI (pasture minus bog). Prater et al. (2006) reported a positive correlation between the Normalized Difference Vegetation Index (NDVI) and ET on post-fire bunchgrass or sagebrush. A positive correlation was also found in upland forests that experience fire (Clark et al., 2012). One possible reason for the non-correlation observed in this study is the lack of transpiration due to burning of vegetation was sufficiently compensated by evaporation with long-lasting precipitation in Period II. Moreover, another reason could be that the influence of other meteorological factors (e.g., $R_n$ and VPD) on ET were not excluded in the correlation between EVI and ET. Subsequently, the results of path analysis showed that EVI had a significant influence on ET only in Period III (coefficient of path b9 in Fig. 7, Table 4). This may be due to the larger fluctuation of LAI in Period III, although there was no clear difference in the observed EVI range among the three periods (Fig. 6d). It was reported that the relationship between EVI and LAI differs depending on vegetation type (e.g., Kang et al., 2016; Qiao et al., 2019). For example, using regression equations between EVI and LAI by Qiao et al. (2019), they reported that the variations in LAI correspond to the variation of EVI (0.25–0.50) and were estimated to be 0.87–2.84, 0.38–2.63, and 0.62–1.94 in deciduous forest, cropland, and grassland, respectively. These estimations would indicate that fluctuation of LAI was larger in woody plants than in herbaceous plants for the same variation of EVI. In period III, woody plants had been dominant, whereas it was sparsely distributed in Periods I and II. Therefore, a significant influence of EVI on ET may be found in Period III because of the large variation in LAI for a certain change in ET.

### 4.5 Low ET sensitivity to VPD after fire

The results of path analysis (Fig. 7) showed that almost no effect of VPD on ET was observed in Period II, whereas VPD affected ET negatively in Periods I and III. This could be explained by the difference in land cover. Previous studies observed the stomatal regulation of fern by showing that their stomatal conductance decreased corresponding to increased VPD (Brodribb and McAdam, 2011; Cardoso et al., 2019; Hõrak et al., 2017; Martins et al., 2016). In our study site, there were fewer herbaceous plants, and some ponds were formed due to large $P$ in Period II. Evaporation from the exposed free water surface increases with an increase in VPD. In contrast, transpiration decreases with increasing VPD due to stomatal closure (e.g., McAdam et al., 2016). These two effects cancel each other out of the VPD change. Furthermore, observed range of $G_s$ was high in Period II comparing with those in Period I and III (Fig. 6e, Table 4). ET does not change much at higher range of $G_s$ ($G_s \geq 10$ mm s$^{-1}$). This might indicate that the rate of increase of ET for $G_s$ was gradual for a higher range of $G_s$ (Fig. 6). This result implies that stomatal regulation for atmospheric dryness became less significant for ET in Period II. This could be an additional reason for the negligible VPD effect in Period II with low VPD and high $G_s$.

### 4.6 ET becomes easier to be decreased due to drainage

Decreased ET under the conditions $P \leq$ ET and GWL< -0.5 (Fig. 3) might be related to the disconnection of capillary force that transfers the water upward. Ishikura et al. (2016) described that the discontinuity of capillary pores is likely to occur in cases with deep GWL. Another possible reason is disabled root water uptake. For example, in boreal poor (weakly minerotrophic) forested fen, most roots lived above -0.4 m soil depth (Dimitrov et al., 2014). The rooting depth of purple moor grass in Dutch peatlands was -0.5 m (Spieksma et al., 1997). From these results, it is inferred that the limitation of root water uptake could be another reason for the decline of ET with GWL< -0.5 m. On the other hand, ET was relatively stable with GWL>-0.5 m even if ET exceeded *P*. Taufik et al. (2017) described that GWL fluctuation influences hydrological drying (or wetting) upper peat layer and the soil moisture is depleted to fulfill the evapotranspiration flux. It could be assumed that shortage of rainwater for ET is compensated with soil water as long as GWL kept above -0.5 m.

In Fig. 4, we can theoretically evaluate underground outflow, which is equivalent to the required water to stabilize the GWL, from x-axis intercept of fitted lines, although head water pressure (i.e., GWL) should be considered for accurate evaluation. We can also evaluate the increasing rate of GWL with unit water supply, which is proportional to soil porosity, from the slope of the fitted lines. Similar fitted lines in Periods I and II as shown in Fig. 4 indicate that the physical properties of soil were not changed by fire in 2009. This may explain the deep soil that was not damaged by fire, although some parts of the peat surface and above ground biomass were burned. The more gradual slope of the fitted line for Period III indicates that a larger amount of water is required to raise a unit GWL. This may be due to the difference in porosity in the range of GWL fluctuation. Specifically, GWL fluctuated in the shallower peat soil layer with lower porosity in Periods I and II, and in the deeper peat soil layer with higher porosity in Period III. In support of this hypothesis, Itoh et al. (2017) reported higher bulk density (corresponding to lower porosity) of peat soil in the shallower layer compared with that in the deeper layer at the study site. The increase in underground outflow in Period III from Period II was estimated at 116 mm month$^{-1}$ from the regression lines as in Fig. 4. Although the estimation was not based on direct measurement, it is confirmed that the underground outflow was increased after canal excavation and the outflow water was as large as the ET at the study site. Therefore, $P$ would become a significant factor to control ET through the change of GWL after canal excavation, as GWL never reached the ground surface level. In contrast, $P$ had generally exceeded the required water volume to maintain the shallowest GWL (i.e., waterlogged condition), at least in the wet season before canal excavation.

Although our study site experienced fire and the vegetation was damaged, water was generally and stably supplied from the peatland to the atmosphere via ET, irrespective of *P*. However, drainage might disable this function because of the available groundwater loss due to deepened GWL resulting from increased underground outflow.

## 4.7 Drainage alters ET sensitivity to GWL

As for the effect of GWL on ET, a small negative effect was found in Period III, whereas the effect was positive in Periods I and II (Fig. 7b). This seems contradictory to the GWL-ET relationship (Fig. 6c) which illustrates the positive relation within the observed range in Periods III. This could be explained that sole GWL-ET relationship would include confounding factors, whereas path analysis excludes the influence of other factors on ET. The small negative effect in Period III could be explained by the following reasons. First, if the GWL is below a certain level where the capillary force is disconnected and root water uptake does not work, transpiration would not be further reduced by GWL deepening. In other words, when the GWL is fluctuating at a deep level, changes in GWL have little effect on ET. In Period III, the GWL was deepened extremely. Second, less rainwater may infiltrate the extremely dried peat soil and evaporation from the peat soil surface may increase. Perdana et al. (2018) reported that peat soil becomes more hydrophobic as it becomes drier. As a result, the duration of the dry period was longer, the GWL deepened, and the peat surface became drier. Specifically, unchanged transpiration and increased evaporation may negatively effect GWL under drier conditions in Period III. Both positive and negative relationships between GWL and ET would also depend on the range of GWL's in boreal peatland bog and pasture (Wang et al., 2020). They explained this complicated relationship by several factors: the impossibility of linear estimation of soil surface moisture by GWL, spatial heterogeneity, and complexity of peat hydrology. Additionally, in Fig. 6c, the fitting curves estimated that ET decreased by 33-69% with GWL drawdown from 0 to 1 m depth. Simultaneously, the same 1 m drawdown decreased ET by 15% in phreatophyte shrubs in arid areas (Nichols, 1994). The rate of decrease in ET for 1 m drawdown was larger at the study site compared with that in the shrub land. Cooper et al. (2006) reported that shrubs have deeper roots than herbaceous plants. These results indicate that ET in herbaceous plant-dominated sites is susceptible to GWL drawdown because of their shallower root depth.

## 5. Conclusions

Fire would have reduced transpiration by burning some of the above-ground vegetation, whereas evaporation from open water contributed to ET in water-logged conditions with subsequent La Niña events. As a result, ET did not decrease immediately after fire. At that time, the effect of reduced transpiration by stomatal closure and increased evaporation from free water surface cancelled each other for atmospheric drying. Additionally, fire-induced haze attenuated incoming solar radiation, then the decrease in $R_n$ reduced ET. On the other hand, drainage could decrease ET. When GWL is deeper than –0.5m, rainwater shortage was not compensated by soil water for stable ET. This would be due to disconnected capillary force and disabled root water uptake. At that time, ET was hardly influenced by GWL fluctuation. Thus, we have shown that fire and drainage potentially reduce ET. However, how much transpiration contributes to ET is not yet well understood. This is very important because transpiration is definitely related to vegetation recovering and which plays a significant role in water cycle or hydrological processes. Therefore, in future research, partitioning ET into evaporation and transpiration would deepen our understanding in such dynamically changing peatland ecosystems.

## Acknowledgement

This study was supported by JSPS Core University Program, JSPS KAKENHI Grant Numbers 13375011, 15255001, 18403001, 21255001, 25257401, and 19H05666, and the JST-JICA Project (SATREPS) (Wild Fire and Carbon Management in Peat-Forest in Indonesia) and Technology Development Fund (no. 2–1504) by the Environmental Restoration and Conservation Agency and the Ministry of the Environment, Japan. We thank the late Dr. Suwido Limin for the site establishment and the staff of CIMTROP, Drs. Yosuke Okimoto, Kiwamu Ishikura, and Masayuki Itoh for their field assistance. We acknowledge the use of data from the FIRMS operated by NASA's Earth Science Data and Information System (ESDIS) with funding provided by NASA Headquarters.

## References

Baker, J. C., & Spracklen, D. V. (2019). Climate benefits of intact Amazon forests and the biophysical consequences of disturbance. *Frontiers in Forests and Global Change*, *2*, 47.

Beringer, J., Hutley, L. B., Tapper, N. J., Coutts, A., Kerley, A., & O'Grady, A. P. (2003). Fire impacts on surface heat, moisture and carbon fluxes from a tropical savanna in northern Australia. *International Journal of Wildland Fire*, *12*(4), 333-340.

Bonan, G. B. (2008). Forests and climate change: forcings, feedbacks, and the climate benefits of forests. *science*, *320*(5882), 1444-1449.

Brodribb, T. J., & McAdam, S. A. (2011). Passive origins of stomatal control in vascular plants. *Science*, *331*(6017), 582-585.

Brust, K., Krebs, M., Wahren, A., Gaudig, G., & Joosten, H. (2018). The water balance of a Sphagnum farming site in north-west Germany. *Mires and Peat*, *20*(10), 1-12.

Cardoso, A. A., Randall, J. M., & McAdam, S. A. (2019). Hydraulics regulate stomatal responses to changes in leaf water status in the fern Athyrium filix-femina. *Plant physiology*, *179*(2), 533-543.

Clark, K. L., Skowronski, N., Gallagher, M., Renninger, H., & Schäfer, K. (2012). Effects of invasive insects and fire on forest energy exchange and evapotranspiration in the New Jersey pinelands. *Agricultural and Forest Meteorology*, *166*, 50-61.

Cooper, D. J., Sanderson, J. S., Stannard, D. I., & Groeneveld, D. P. (2006). Effects of long-term water table drawdown on evapotranspiration and vegetation in an arid region phreatophyte community. *Journal of Hydrology*, *325*(1-4), 21-34.

D'Acunha, B., Lee, S. C., & Johnson, M. S. (2018). Ecohydrological responses to rewetting of a highly impacted raised bog ecosystem. *Ecohydrology*, *11*(1), e1922.

Dimitrov, D. D., Bhatti, J. S., & Grant, R. F. (2014). The transition zones (ecotone) between boreal forests and peatlands: Ecological controls on ecosystem productivity along a transition zone between upland black spruce forest and a poor forested fen in central Saskatchewan. *Ecological modelling*, *291*, 96-108.

Fisher, J. B., Malhi, Y., Bonal, D., Da Rocha, H. R., De Araujo, A. C., Gamo, M., ... & Kumagai, T. O. (2009). The land–atmosphere water flux in the tropics. *Global Change Biology*, *15*(11), 2694-2714.

Foken, T., & Wichura, B. (1996). Tools for quality assessment of surface-based flux measurements. *Agricultural and forest meteorology*, *78*(1-2), 83-105.

Foken, T. (2017). Experimental methods for estimating the fluxes of energy and matter. In *Micrometeorology* (pp. 143-205). Springer, Berlin, Heidelberg.

Fraser, C. J. D., Roulet, N. T., & Lafleur, M. (2001). Groundwater flow patterns in a large peatland. *Journal of Hydrology*, *246*(1-4), 142-154.

Hirano, T., Kusin, K., Limin, S., & Osaki, M. (2014). Carbon dioxide emissions through oxidative peat decomposition on a burnt tropical peatland. *Global change biology*, *20*(2), 555-565.

Hirano, T., Kusin, K., Limin, S., & Osaki, M. (2015). Evapotranspiration of tropical peat swamp forests. *Global change biology*, *21*(5), 1914-1927.

Hõrak, H., Kollist, H., & Merilo, E. (2017). Fern stomatal responses to ABA and CO2 depend on species and growth conditions. *Plant Physiology*, *174*(2), 672-679.

Huijnen, V., Wooster, M. J., Kaiser, J. W., Gaveau, D. L., Flemming, J., Parrington, M., ... & Van Weele, M. (2016). Fire carbon emissions over maritime southeast Asia in 2015 largest since 1997. *Scientific reports*, *6*, 26886.

Ishikura, K., Yamada, H., Toma, Y., Takakai, F., Morishita, T., Darung, U., ... & Hatano, R. (2017). Effect of groundwater level fluctuation on soil respiration rate of tropical peatland in Central Kalimantan, Indonesia. *Soil science and plant nutrition*, *63*(1), 1-13.

Ismanto, H., Hartono, H., & Marfai, M. A. (2019). Spatiotemporal visibility characteristics impacted by forest and land fire over airports in sumatera and borneo Island, Indonesia. *Quaestiones Geographicae*, *38*(3), 5-16.

Itoh, M., Okimoto, Y., Hirano, T., & Kusin, K. (2017). Factors affecting oxidative peat decomposition due to land use in tropical peat swamp forests in Indonesia. *Science of the Total Environment*, *609*, 906-915.

Jarvis, P. G., & McNaughton, K. G. (1986). Stomatal control of transpiration: scaling up from leaf to region. In *Advances in ecological research* (Vol. 15, pp. 1-49). Academic Press.

Kang, Y., Özdoğan, M., Zipper, S. C., Román, M. O., Walker, J., Hong, S. Y., ... & Loheide, S. P. (2016). How universal is the relationship between remotely sensed vegetation indices and crop leaf area index? A global assessment. *Remote sensing*, *8*(7), 597.

Kettridge, N., Lukenbach, M. C., Hokanson, K. J., Hopkinson, C., Devito, K. J., Petrone, R. M., ... & Waddington, J. M. (2017). Low evapotranspiration enhances the resilience of peatland carbon stocks to fire. *Geophysical Research Letters*, *44*(18), 9341-9349.

Kettridge, N., Lukenbach, M. C., Hokanson, K. J., Devito, K. J., Petrone, R. M., Mendoza, C. A., & Waddington, J. M. (2019). Severe wildfire exposes remnant peat carbon stocks to increased post-fire drying. *Scientific reports*, *9*(1), 1-6.

Kumagai, T., Saitoh, T. M., Sato, Y., Takahashi, H., Manfroi, O. J., Morooka, T., ... &

Komatsu, H. (2005). Annual water balance and seasonality of evapotranspiration in a Bornean tropical rainforest. *Agricultural and Forest Meteorology*, *128*(1-2), 81-92.

Kume, T., Tanaka, N., Kuraji, K., Komatsu, H., Yoshifuji, N., Saitoh, T. M., ... & Kumagai, T. O. (2011). Ten-year evapotranspiration estimates in a Bornean tropical rainforest. *Agricultural and Forest Meteorology*, *151*(9), 1183-1192.

Lafleur, P. M. (2008). Connecting atmosphere and wetland: energy and water vapour exchange. *Geography Compass*, *2*(4), 1027-1057.

Liu, H., Randerson, J. T., Lindfors, J., & Chapin III, F. S. (2005). Changes in the surface energy budget after fire in boreal ecosystems of interior Alaska: An annual perspective. *Journal of Geophysical Research: Atmospheres*, *110*(D13).

Longo, M., Saatchi, S., Keller, M., Bowman, K., Ferraz, A., Moorcroft, P. R., ... & Vincent, G. (2020). Impacts of degradation on water, energy, and carbon cycling of the Amazon tropical forests. *Journal of Geophysical Research: Biogeosciences*, *125*(8), e2020JG005677.

Martins, S. C., McAdam, S. A., Deans, R. M., DaMatta, F. M., & Brodribb, T. J. (2016). Stomatal dynamics are limited by leaf hydraulics in ferns and conifers: results from simultaneous measurements of liquid and vapour fluxes in leaves. *Plant, cell & environment*, *39*(3), 694-705.

Massman, W. J. (2000). A simple method for estimating frequency response corrections for eddy covariance systems. *Agricultural and Forest Meteorology*, *104*(3), 185-198.

Massman, W. J. (2001). Reply to comment by Rannik on" A simple method for estimating frequency response corrections for eddy covariance systems". *Agricultural and Forest Meteorology. 107: 247-251.*, *107*, 247-251.

McAdam, S. A., Sussmilch, F. C., & Brodribb, T. J. (2016). Stomatal responses to vapour pressure deficit are regulated by high speed gene expression in angiosperms. *Plant, cell & environment*, *39*(3), 485-491.

Mezbahuddin, M., Grant, R. F., & Hirano, T. (2015). How hydrology determines seasonal and interannual variations in water table depth, surface energy exchange, and water stress in a tropical peatland: Modeling versus measurements. *Journal of Geophysical Research: Biogeosciences*, *120*(11), 2132-2157.

Miettinen, J., Shi, C., & Liew, S. C. (2016). Land cover distribution in the peatlands of Peninsular Malaysia, Sumatra and Borneo in 2015 with changes since 1990. *Global Ecology and Conservation*, *6*, 67-78.

Montes-Helu, M. C., Kolb, T., Dore, S., Sullivan, B., Hart, S. C., Koch, G., & Hungate, B. A. (2009). Persistent effects of fire-induced vegetation change on energy partitioning and evapotranspiration in ponderosa pine forests. *agricultural and forest* *meteorology*, *149*(3-4), 491-500.

Moore, P. A., Pypker, T. G., & Waddington, J. M. (2013). Effect of long-term water table manipulation on peatland evapotranspiration. *Agricultural and Forest Meteorology*, *178*, 106-119.

Morison, M. Q., Petrone, R. M., Wilkinson, S. L., Green, A., & Waddington, J. M. (2020). Ecosystem scale evapotranspiration and $CO_2$ exchange in burned and unburned peatlands: Implications for the ecohydrological resilience of carbon stocks to wildfire. *Ecohydrology*, *13*(2), e2189.

Nichols, W. D. (1994). Groundwater discharge by phreatophyte shrubs in the Great Basin as related to depth to groundwater. *Water Resources Research*, *30*(12), 3265-3274.

Ohkubo, S., Hirano, T., & Kusin, K. (2021a). Influence of disturbances and environmental changes on albedo in tropical peat ecosystems. *Agricultural and Forest Meteorology*, *301*, 108348.

Ohkubo, S., Hirano, T., & Kusin, K. (2021b). Assessing the carbon dioxide balance of a degraded tropical peat swamp forest following multiple fire events of different intensities. *Agricultural and Forest Meteorology*, *306*, 108448.

Page, S. E., Rieley, J. O., & Banks, C. J. (2011). Global and regional importance of the tropical peatland carbon pool. *Global change biology*, *17*(2), 798-818.

Perdana, L. R., Ratnasari, N. G., Ramadhan, M. L., Palamba, P., & Nugroho, Y. S. (2018, January). Hydrophilic and hydrophobic characteristics of dry peat. In *IOP Conference Series: Earth and Environmental Science* (Vol. 105, No. 1, p. 012083). IOP Publishing Ltd..

Petrone, R. M., Price, J. S., Waddington, J. M., & Von Waldow, H. (2004). Surface moisture and energy exchange from a restored peatland, Quebec, Canada. *Journal of Hydrology*, *295*(1-4), 198-210.

Prater, M. R., & DeLucia, E. H. (2006). Non-native grasses alter evapotranspiration and energy balance in Great Basin sagebrush communities. *Agricultural and Forest Meteorology*, *139*(1-2), 154-163.

Qiao, K., Zhu, W., Xie, Z., & Li, P. (2019). Estimating the seasonal dynamics of the leaf area index using piecewise LAI-VI relationships based on phenophases. *Remote Sensing*, *11*(6), 689.

Sottocornola, M., & Kiely, G. (2010). Energy fluxes and evaporation mechanisms in an Atlantic blanket bog in southwestern Ireland. *Water resources research*, *46*(11).

Spieksma, J. F. M., Moors, E. J., Dolman, A. J., & Schouwenaars, J. M. (1997). Modelling evaporation from a drained and rewetted peatland. *Journal of* *hydrology*, *199*(3-4), 252-271.

Sun, L., Song, C., Lafleur, P. M., Miao, Y., Wang, X., Gong, C., ... & Tan, W. (2018). Wetland-atmosphere methane exchange in Northeast China: A comparison of permafrost peatland and freshwater wetlands. *Agricultural and forest meteorology*, *249*, 239-249.

Taufik, M., Torfs, P. J., Uijlenhoet, R., Jones, P. D., Murdiyarso, D., & Van Lanen, H. A. (2017). Amplification of wildfire area burnt by hydrological drought in the humid tropics. *Nature Climate Change*, *7*(6), 428-431.

Twine, T. E., Kustas, W. P., Norman, J. M., Cook, D. R., Houser, P., Meyers, T. P., ... & Wesely, M. L. (2000). Correcting eddy-covariance flux underestimates over a grassland. *Agricultural and forest meteorology*, *103*(3), 279-300.

Ueyama, M., Hirata, R., Mano, M., Hamotani, K., Harazono, Y., Hirano, T., ... & Takahashi, Y. (2012). Influences of various calculation options on heat, water and carbon fluxes determined by open-and closed-path eddy covariance methods. *Tellus B: Chemical and Physical Meteorology*, *64*(1), 19048.

Valentini, R., Dore, S., Marchi, G., Mollicone, D., Panfyorov, M., Rebmann, C., ... & Schulze, E. D. (2000). Carbon and Water Exchanges of Two Constrasting Central Siberia Landscape Types: Regenerating Forest and Bog. *Functional ecology*, 87-96.

Vickers, D., & Mahrt, L. (1997). Quality control and flux sampling problems for tower and aircraft data. *Journal of atmospheric and oceanic technology*, *14*(3), 512-526.

Wang, M., Wu, J., & Lafleur, P. (2020). Comparison of energy fluxes between an undisturbed bog and an adjacent abandoned peatland pasture. *Agricultural and Forest Meteorology*, *291*, 108086.

Webb, E. K., Pearman, G. I., & Leuning, R. (1980). Correction of flux measurements for density effects due to heat and water vapour transfer. *Quarterly Journal of the Royal Meteorological Society*, *106*(447), 85-100.

Whelan, A., Starr, G., Staudhammer, C. L., Loescher, H. W., & Mitchell, R. J. (2015). Effects of drought and prescribed fire on energy exchange in longleaf pine ecosystems. *Ecosphere*, *6*(7), 1-22.

Wilkinson, S. L., Verkaik, G. J., Moore, P. A., & Waddington, J. M. (2020). Threshold peat burn severity breaks evaporation-limiting feedback. *Ecohydrology*, *13*(1), e2168.

Wu, J., Kutzbach, L., Jager, D., Wille, C., & Wilmking, M. (2010). Evapotranspiration dynamics in a boreal peatland and its impact on the water and energy balance. *Journal of Geophysical Research: Biogeosciences*, *115*(G4).

## Figure legends

Fig. 1 Locations of the study site in Central Kalimantan, Indonesia.

Fig. 2 Monthly variations in (a) $P$ and ET, (b) GWL, (c) VPD, (d) energy fluxes, (e) $\beta$, and (f) $G_s$ and $\Omega$, along with (f) EVI at 16-days intervals. Monthly SOI is shown at the bottom (h). $P$ (blue bars) and ET (red bars) are displayed over each other (i.e., overlapped volume are displayed by purple). EVI data were classified into two ranks according to reliability: useful or better (solid circles) and others (open circles). The red line denotes a moving average of seven consecutive points excluding low-ranked data. Vertical dashed lines indicate the borders of Period I, II and III. Two triangles in the uppermost graph indicate the moment when the measurement height was changed.

Fig. 3 Relationship between ET and $P$ observed on monthly basis. Data were classified into three observation periods: Period I (black), Period II (red), and Period III (green). The data with $-0.5 \leq$GWL$< -0.3$ m and GWL$< -0.5$ m are indicated by triangle and cross, respectively.

Fig. 4 Relationship between monthly change in GWL (ΔGWL) and $P$−ET. The data with GWL$< -0.1$ m were selected to exclude the contribution of surface outflow. Data classification was same as in Fig. 3.

Fig. 5 Relationship between daytime $\beta$ and $R_n$ (a) or VPD in case of $R_n \geq 600$ (b). Half-hourly data with $R_n > 0$ are binned into 10 classes of $R_n$ (a) or VPD in case of $R_n \geq 600$ (b) in each Period I, II and III. The average of $\beta$ with standard deviation in each class are illustrated by circles with error bars.

Fig. 6 Relationship between ET and environmental factors: (a) $R_n$, (b) VPD, (c) GWL, (d) EVI, (e) $G_s$, and (f) $\Omega$. Half-hourly ET are binned into 20 classes of each environmental factor except the case that monthly ET was used with EVI. The average of ET with standard deviation in each class are illustrated by circles with error bars.

Fig. 7 (a) Path diagram of ET. (b) Total effect of $P$, $R_n$, VPD, GWL, and EVI on ET, determined with standardized path coefficients. Analyses were conducted using monthly data for three periods (Period I, II and III) and whole observation period.

**Abstract:**

Tropical peat swamp forests (PSFs) play a significant role in the exchange of water between land and the atmosphere. However, fire and drainage have been expanding in PSFs in recent decades. Although there is concern on the influence of fire and drainage on water circulation, their influence on evapotranspiration (ET) is insufficiently understood. Furthermore, repeated fire occurrences and their corresponding influence on the ET by recurrent burning and smoldering is unexplored. To elucidate these influences, we examined long-term variation of ET in a degraded peat swamp forest in Central Kalimantan, Indonesia that was affected by drainage and repeated fire. The continuous observation of energy fluxes was conducted for approximately 13 years between 2004 and 2016 by using the eddy covariance technique. The site burned in 2009 and 2014, and was drained in 2014. Monthly ET and net radiation ($R_n$) fluctuated in synchrony and thus they decreased considerably under fire-induced dense haze during the El Niño drought. Troughs of ET, groundwater level (GWL) and $R_n$ and crests of vapor pressure deficit (VPD) coincided in their time-series variations. In the case of ET > precipitation ($P$), ET decreased when the GWL was deeper than -0.5 m. Half-hourly ET had a strong positive correlation with $R_n$ ($R$=0.89, $p$ <0.01), and partial positive relationship with VPD when VPD<20 hPa and with GWL when GWL<-0.5 m. ET had no correlation with the

Enhanced Vegetation Index (EVI), which represents above ground biomass for the entire observation period. Alternately, the results of path analysis showed that some environmental factors controlled ET differently depending on environmental conditions. Generally, VPD negatively affected ET due to stomatal regulation functions under dry atmospheric conditions. However, the effect was negligible during the water-logged periods. This is because atmospheric dryness facilitated evaporation from exposed water on the ground surface, which canceled out the negative effect of transpiration due to stomatal closure. After drainage by canal excavation, fluctuation of GWL did not significantly influence ET, although ET decreased. This may be due to the hydrophobic dried peat soil, which prevents rainwater infiltration, disconnection of capillary force, or disabled root water uptake as GWL excessively deepened. Fire potentially decreased ET due to decreased transpiration by burning of vegetation. However, the decreasing effect was cancelled by increased evaporation from the waterlogged ground surface during the subsequent La Niña event. Drainage undoubtedly deepened the GWL, and ET severely decreased in cases with extremely deep GWL.

Table 1

Characteristics of each period.

| Period | Term | Characteristics |
|---|---|---|
| I | May 2004–September 2009 | Herbaceous plants dominated. |
| II | December 2009–June 2014 | Vegetation rapidly recovered after fire.<br>Water-logged condition lasted for a long term. |
| III | July 2014–October 2016 | Woody plants have become dominant.<br>Severe haze occurred in 2014 and 2015. |

Table 2

Annual values of ET and environmental factors.

| Year | 2005 | 2006 | 2007 | 2008 | 2009 | 2010 | 2011 | 2012 | 2013 | 2014 | 2015 | 2016 | Mean ± sd. |
|---|---|---|---|---|---|---|---|---|---|---|---|---|---|
| (Period) | (I) | (I) | (I) | (I) | (I / II) | (II) | (II) | (II) | (II) | (II / III) | (III) | (III) | |
| ET (mm yr$^{-1}$) | 1494 | 1271 | 1434 | 1353 | 1357[a] | 1662 | 1613 | 1630 | 1648 | 1374 | 1222 | 1426[a] | 1457 ± 152 |
| | (1234) | (1098) | (1169) | (966) | (1020) | (1271) | (1328) | (1318) | (1329) | (1175) | (1076) | (1222) | (1184 ± 122) |
| $P$ (mm yr$^{-1}$) | 2620 | 1977 | 2555 | 2603 | 2239[d] | 3750 | 3021 | 2460 | 2776 | 2220 | 2388 | 3077[d] | 2641 ± 474 |
| ET/$P$ | 0.57 | 0.64 | 0.56 | 0.52 | 0.61[a] | 0.44 | 0.53 | 0.66 | 0.59 | 0.61 | 0.51 | 0.46[a] | 0.56 ± 0.07 |
| GWL (m) | −0.08 | −0.25 | 0.00 | −0.03 | −0.19[b] | 0.01 | −0.04 | −0.08 | −0.06 | −0.22 | −0.59 | −0.42[c] | −0.16 ± 0.18 |
| $R_n$ (GJ m$^{-2}$ yr$^{-1}$) | 4.54 | 4.13 | 4.67 | 4.58 | 4.53[b] | 4.91 | 4.90 | 4.89 | 4.98 | 4.45 | 4.06 | 4.46[a] | 4.59 ± 0.30 |
| $H$ (GJ m$^{-2}$ yr$^{-1}$) | 0.76 | 0.90 | 0.97 | 0.92 | 0.96[a] | 0.66 | 0.80 | 0.75 | 0.79 | 0.98 | 0.96 | 0.81[a] | 0.86 ± 0.10 |

| | | | | | | | | | | | | | |
|---|---|---|---|---|---|---|---|---|---|---|---|---|---|
| $\lambda E$ (GJ m$^{-2}$ yr$^{-1}$) | 3.00 | 2.67 | 2.84 | 2.35 | 2.47[a] | 3.09 | 3.23 | 3.20 | 3.23 | 2.85 | 2.61 | 2.97[a] | 2.88 ± 0.30 |
| $\beta$ | 0.25 | 0.34 | 0.34 | 0.39 | 0.39[a] | 0.22 | 0.25 | 0.23 | 0.25 | 0.37 | 0.36 | 0.28[a] | 0.31 ± 0.07 |
| VPD (hPa) | 6.95 | 7.42 | 7.20 | 6.79 | 7.75[b] | 6.00 | 6.43 | 6.36 | 6.22 | 7.60 | 7.74 | 6.21 | 6.89 ± 0.64 |
| $G_s$ (mm s$^{-1}$) | 9.33 | 7.55 | 8.78 | 7.89 | 7.37[a] | 11.33 | 10.02 | 10.39 | 10.57 | 8.50 | 6.36 | 9.10[a] | 8.93 ± 1.48 |
| $\Omega$ | 0.65 | 0.45 | 0.52 | 0.59 | 0.56[a] | 0.72 | 0.68 | 0.68 | 0.67 | 0.55 | 0.52 | 0.65[a] | 0.60 ± 0.08 |
| EVI | 0.42 | 0.43 | 0.41 | 0.43 | 0.39 | 0.29 | 0.36 | 0.41 | 0.44 | 0.36 | 0.35 | 0.41 | 0.40 ± 0.04 |

Uncorrected ETs without energy balance closure are shown in parentheses.

[a] Including consecutive gap-filled data for more than one month.

[b] Including data gaps for approximately 2.5 months.

[c] Including data gaps for approximately 1 month.

[d] Data gaps for approximately 2.5 months were filled with the data measured at a nearby forest site.

Table 3

Mean monthly values of ET and environmental factors. Uncorrected ETs without energy balance closure are shown in parentheses. The $p$ values of one-way ANOVA are listed in the extreme-right column. Different letters in the same row denote significant difference ($p<0.05$) among the three periods according to Tukey's HSD.

| | Period I | Period II | Period III | ANOVA ($p$) |
|---|---|---|---|---|
| ET (mm $\text{month}^{-1}$) | 119 ± 15 a | 136 ± 9 b | 109 ± 22 c | <0.001 |
| | (97 ± 13) | (109 ± 9) | (95 ± 17) | |
| $P$ (mm $\text{month}^{-1}$) | 191 ± 135 a | 253 ± 121 b | 206 ± 151 ab | 0.041 |
| ET/$P$ | 0.62 | 0.54 | 0.53 | |
| GWL (m) | −0.13 ± 0.27 a | −0.04 ± 0.10 a | −0.50 ± 0.30 b | <0.001 |
| $R_n$ (MJ $\text{m}^{-2}$ $\text{month}^{-1}$) | 376 ± 37 a | 407 ± 26 b | 354 ± 67 a | <0.001 |

| | | | | |
|---|---|---|---|---|
| $H$ (MJ m$^{-2}$ month$^{-1}$) | 74 ± 24 a | 62 ± 11 b | 79 ± 23 a | <0.001 |
| $\lambda E$ (MJ m$^{-2}$ month$^{-1}$) | 235 ± 31 a | 265 ± 22 b | 231 ± 42 a | <0.001 |
| $\beta$ | 0.32 | 0.23 | 0.34 | |
| VPD (hPa) | 7.26 ± 1.30 a | 6.27 ± 1.02 b | 7.51 ± 1.73 a | <0.001 |
| $G_s$ (mm s$^{-1}$) | 8.14 ± 2.38 a | 10.76 ± 1.65 b | 7.31 ± 2.32 a | <0.001 |
| $\Omega$ | 0.62 ± 0.11 a | 0.69 ± 0.04 b | 0.56 ± 0.10 c | <0.001 |
| EVI | 0.41 ± 0.05 a | 0.38 ± 0.06 b | 0.39 ± 0.07 ab | 0.020 |

Mean ± 1 standard deviation

Table 4

Standardized path coefficients of path diagram (Fig. 6a) for each period. The significant level is denoted by * for $p < 0.05$ and ** for $p < 0.01$.

| Path | Period I | Period II | Period III | Whole period |
|---|---|---|---|---|
| b1 | −0.22 | 0.10 | 0.10 | 0.10 |
| b2 | 0.31** | 0.02 | 0.52** | 0.47** |
| b3 | 0.08 | 0.37* | 0.38** | 0.15* |
| b4 | −0.82** | −0.57** | −0.28* | −0.52** |
| b5 | −0.70** | −0.34** | −0.59** | −0.54** |
| b6 | 0.62** | 0.87** | 0.97** | 0.80** |
| b7 | 0.35 | 0.34** | −0.09 | 0.15** |
| b8 | −0.34 | 0.24** | −0.29** | −0.18** |
| b9 | −0.17 | 0.11 | 0.18** | 0.08* |
| GFI | 0.88 | 0.86 | 0.89 | 0.96 |

Table S1

Summary of energy balance closure. Values were determined with the observed half hourly data in each year. The slopes, intercepts, and coefficient of determination ($R^2$) were determined by linear regression between $R_n$ (x-axis) and $H+\lambda E$ (y-axis). $(H+\lambda E)/R_n$ were annual averages of each year.

| Year | Slope | Intercept (W m$^{-2}$) | $R^2$ | $(H+\lambda E)/R_n$ |
|---|---|---|---|---|
| 2004 | 0.54 | 40.8 | 0.80 | 0.66 |
| 2005 | 0.55 | 45.2 | 0.76 | 0.70 |
| 2006 | 0.62 | 23.8 | 0.84 | 0.72 |
| 2007 | 0.59 | 27.8 | 0.88 | 0.72 |
| 2008 | 0.48 | 35.2 | 0.81 | 0.65 |
| 2009 | 0.65 | 29.4 | 0.86 | 0.74 |
| 2010 | 0.57 | 33.6 | 0.81 | 0.68 |
| 2011 | 0.62 | 41.2 | 0.76 | 0.75 |
| 2012 | 0.67 | 27.9 | 0.84 | 0.75 |
| 2013 | 0.71 | 20.7 | 0.85 | 0.77 |
| 2014 | 0.73 | 23.3 | 0.85 | 0.80 |
| 2015 | 0.73 | 29.2 | 0.81 | 0.83 |

| | | | | |
|---|---|---|---|---|
| 2016 | 0.75 | 13.2 | 0.85 | 0.81 |
| Mean ± 1SD | 0.63 ± 0.08 | 30.5 ± 8.3 | 0.82 ± 0.04 | 0.74 ± 0.06 |

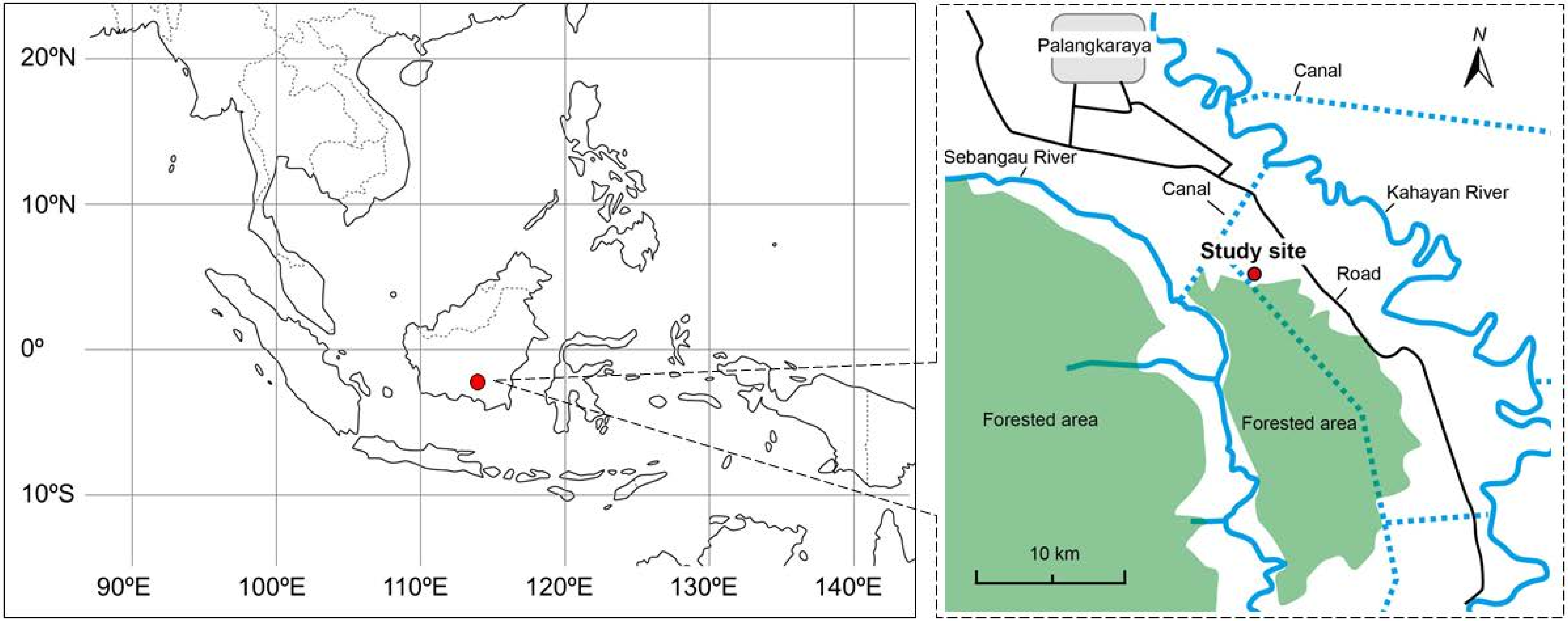
20ºN
10ºN
0º
10ºS
90ºE
100ºE
110ºE
120ºE
130ºE
140ºE
Palangkaraya
N
Canal
Sebangau River
Canal
Kahayan River
Study site
Road
Forested area
Forested area
10 km

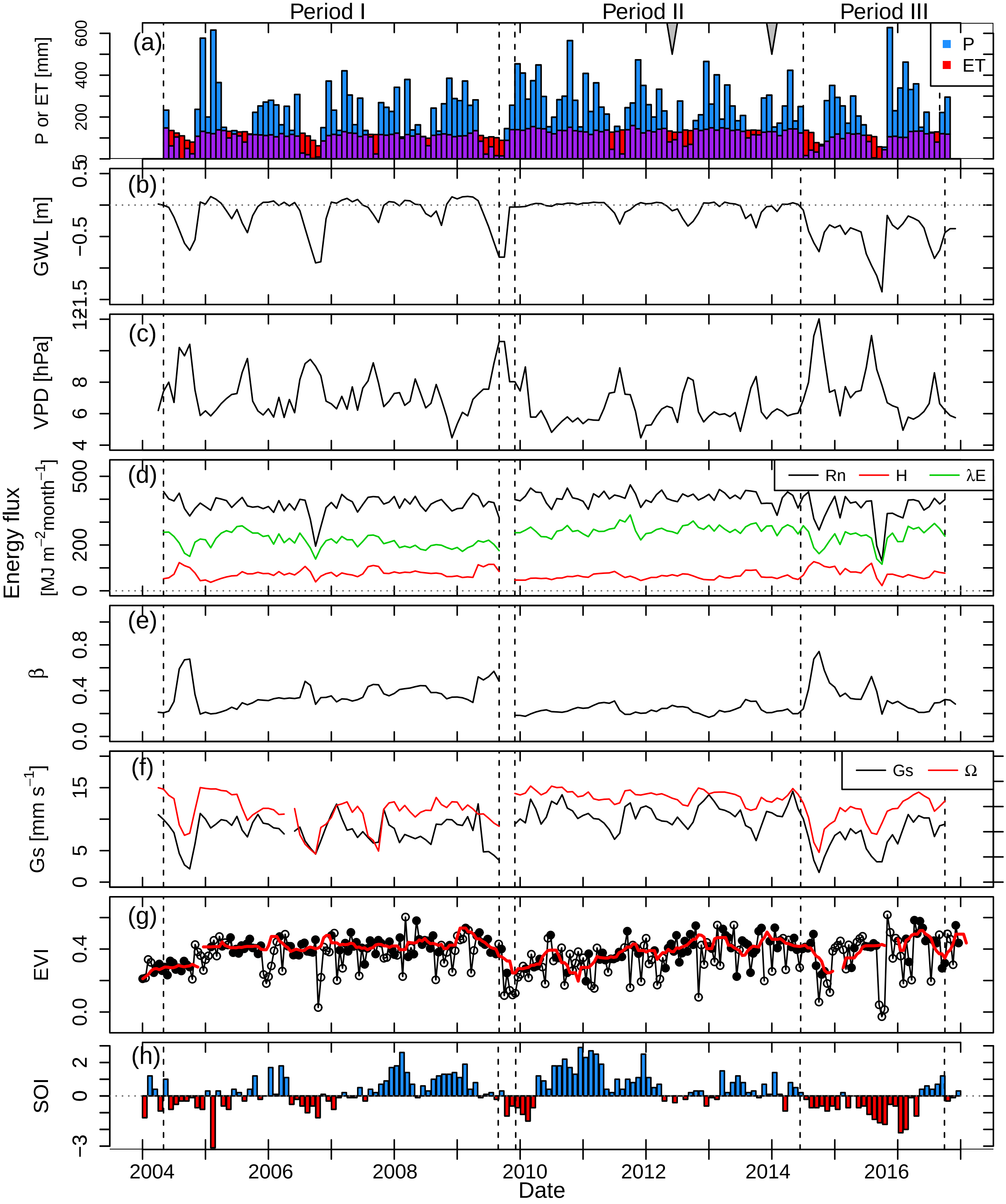
Period I
Period II
Period III
(a)
P or ET [mm]
0
200
400
600
P
ET
(b)
GWL [m]
0.5
−0.5
−1.5
(c)
VPD [hPa]
4
6
8
10
12
(d)
Energy flux
[MJ m$^{-2}$month$^{-1}$]
0
200
500
Rn
H
λE
(e)
β
0.0
0.4
0.8
(f)
Gs [mm s$^{-1}$]
0
5
15
Gs
Ω
0.0
0.4
0.8
(g)
EVI
0.0
0.4
(h)
SOI
−3
0
2
2004
2006
2008
2010
2012
2014
2016
Date

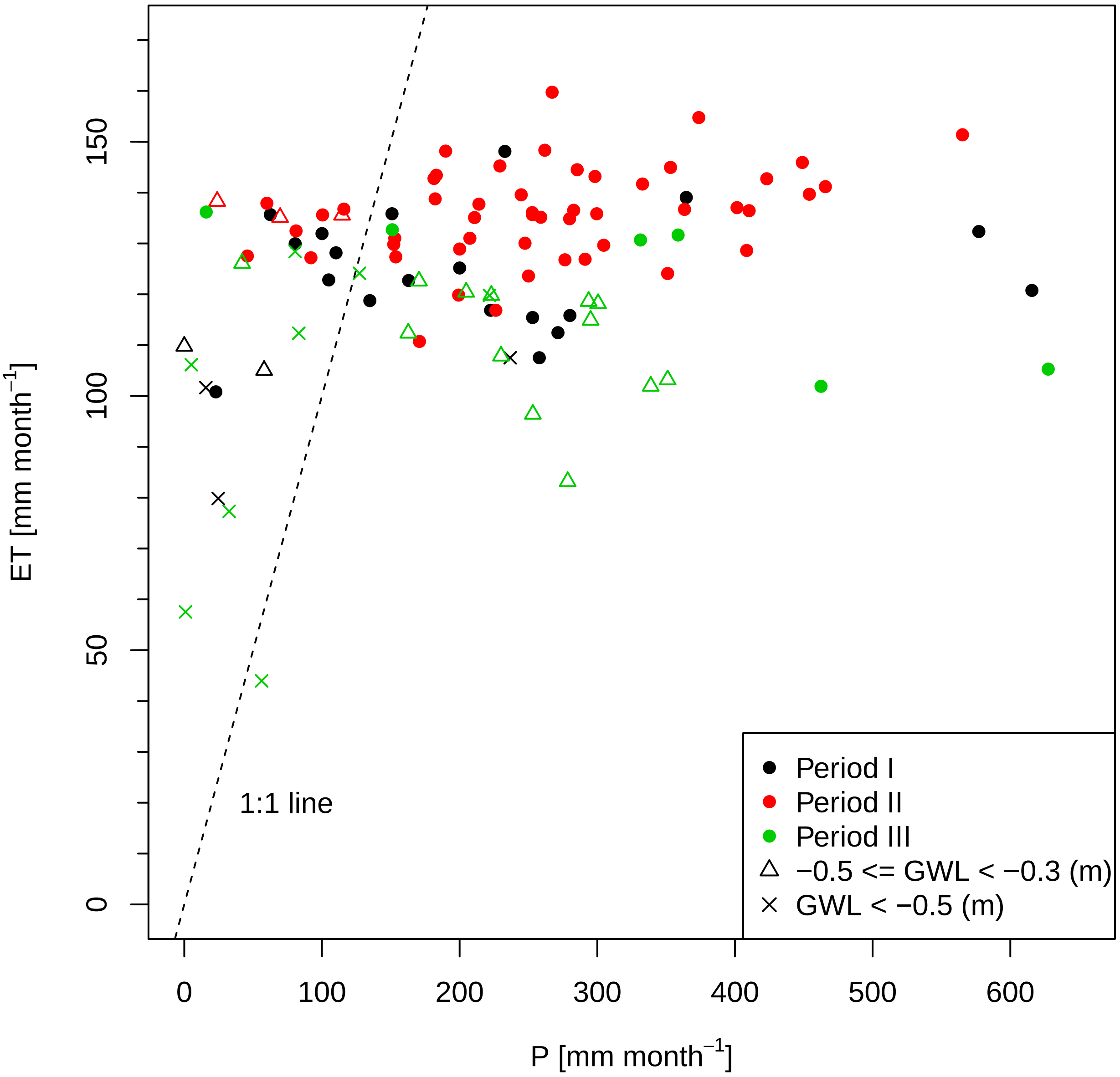
ET [mm month$^{-1}$]
P [mm month$^{-1}$]
0
50
100
150
0
100
200
300
400
500
600
1:1 line
Period I
Period II
Period III
−0.5 <= GWL < −0.3 (m)
GWL < −0.5 (m)

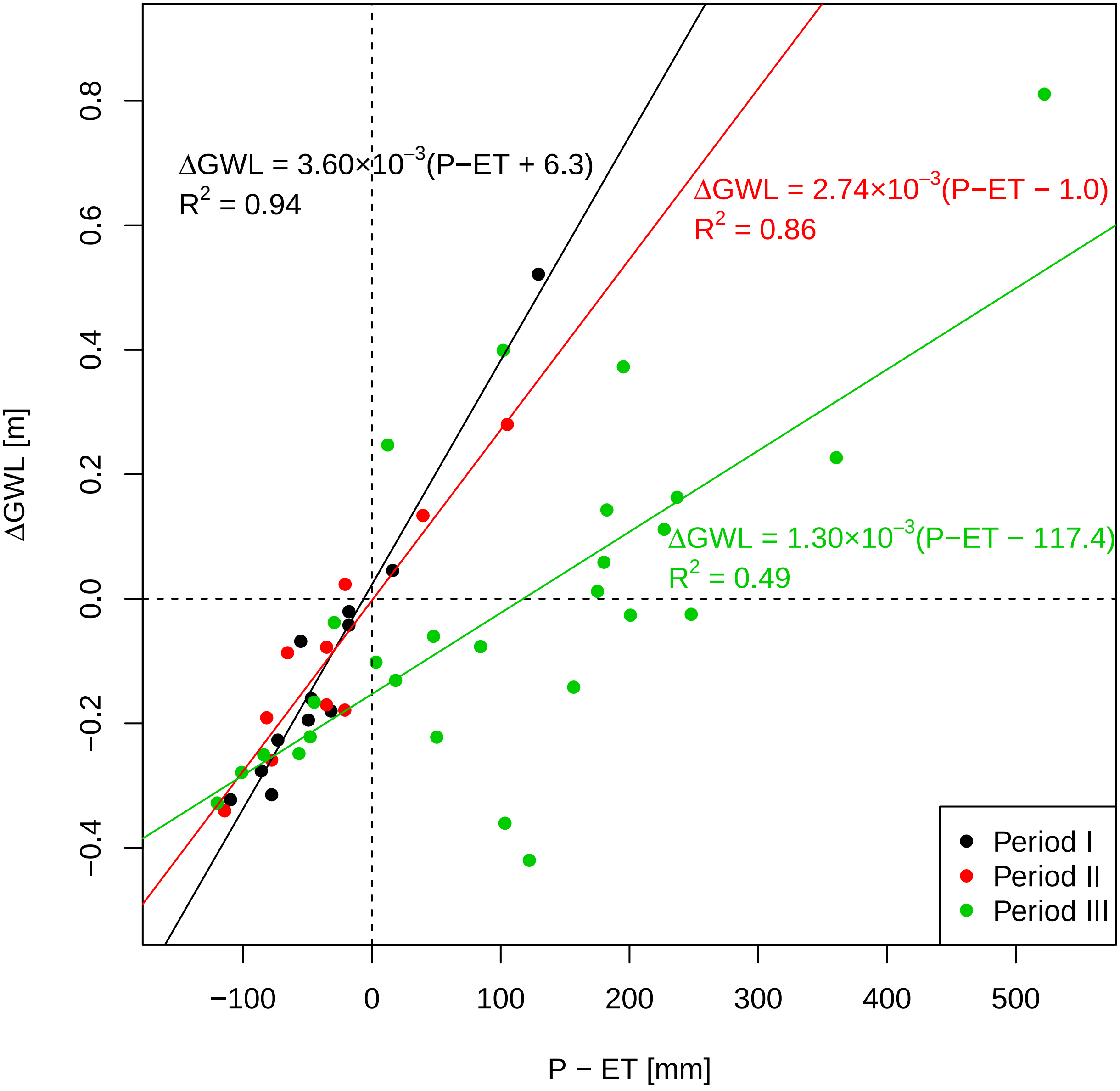
ΔGWL = 3.60×10$^{-3}$(P−ET + 6.3)
R$^2$ = 0.94
ΔGWL = 2.74×10$^{-3}$(P−ET − 1.0)
R$^2$ = 0.86
ΔGWL = 1.30×10$^{-3}$(P−ET − 117.4)
R$^2$ = 0.49
ΔGWL [m]
0.8
0.6
0.4
0.2
0.0
−0.2
−0.4
−100
0
100
200
300
400
500
P − ET [mm]
● Period I
● Period II
● Period III

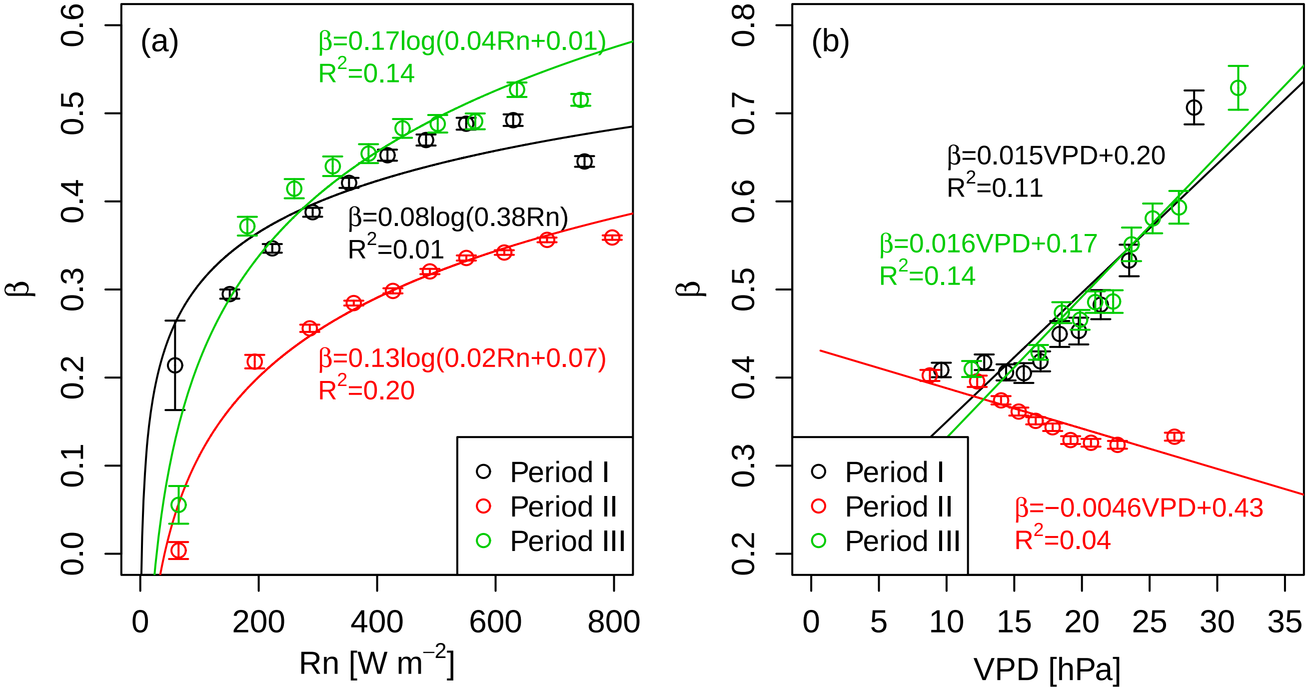
(a)
β=0.17log(0.04Rn+0.01)
R2=0.14
β=0.08log(0.38Rn)
R2=0.01
β=0.13log(0.02Rn+0.07)
R2=0.20
Period I
Period II
Period III
β
0.0
0.1
0.2
0.3
0.4
0.5
0.6
0
200
400
600
800
Rn [W m−2]
(b)
β=0.015VPD+0.20
R2=0.11
β=0.016VPD+0.17
R2=0.14
β=−0.0046VPD+0.43
R2=0.04
Period I
Period II
Period III
β
0.2
0.3
0.4
0.5
0.6
0.7
0.8
0
5
10
15
20
25
30
35
VPD [hPa]

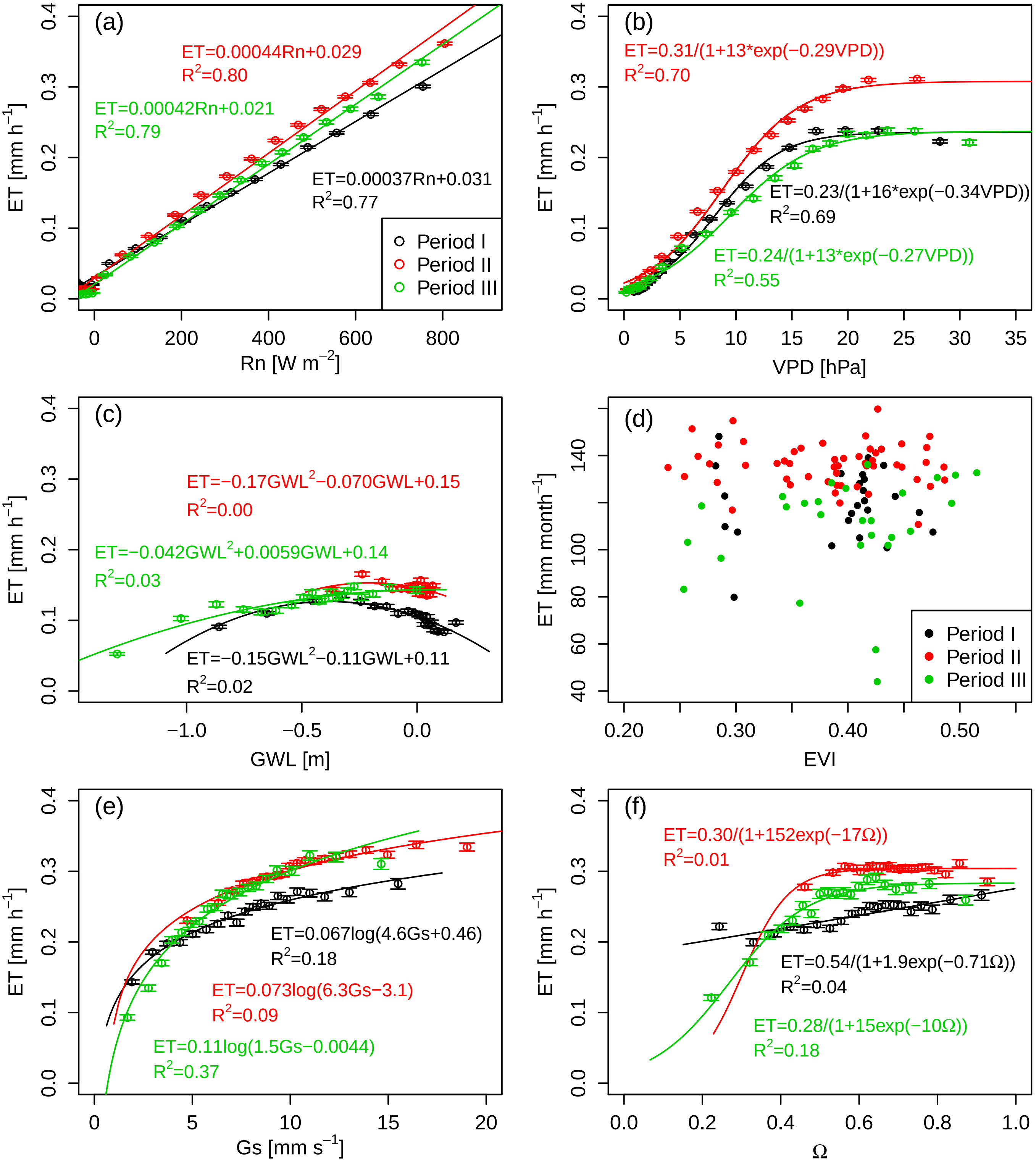
(a)
ET=0.00044Rn+0.029
$R^2$=0.80
ET=0.00042Rn+0.021
$R^2$=0.79
ET=0.00037Rn+0.031
$R^2$=0.77
Period I
Period II
Period III
ET [mm $h^{-1}$]
Rn [W $m^{-2}$]
0.0
0.1
0.2
0.3
0.4
0
200
400
600
800
(b)
ET=0.31/(1+13*exp(−0.29VPD))
$R^2$=0.70
ET=0.23/(1+16*exp(−0.34VPD))
$R^2$=0.69
ET=0.24/(1+13*exp(−0.27VPD))
$R^2$=0.55
ET [mm $h^{-1}$]
VPD [hPa]
0
5
10
15
20
25
30
35
(c)
ET=−0.17$GWL^2$−0.070GWL+0.15
$R^2$=0.00
ET=−0.042$GWL^2$+0.0059GWL+0.14
$R^2$=0.03
ET=−0.15$GWL^2$−0.11GWL+0.11
$R^2$=0.02
ET [mm $h^{-1}$]
GWL [m]
−1.0
−0.5
0.0
(d)
Period I
Period II
Period III
ET [mm $month^{-1}$]
EVI
40
60
80
100
140
0.20
0.30
0.40
0.50
(e)
ET=0.067log(4.6Gs+0.46)
$R^2$=0.18
ET=0.073log(6.3Gs−3.1)
$R^2$=0.09
ET=0.11log(1.5Gs−0.0044)
$R^2$=0.37
ET [mm $h^{-1}$]
Gs [mm $s^{-1}$]
0
5
10
15
20
(f)
ET=0.30/(1+152exp(−17Ω))
$R^2$=0.01
ET=0.54/(1+1.9exp(−0.71Ω))
$R^2$=0.04
ET=0.28/(1+15exp(−10Ω))
$R^2$=0.18
ET [mm $h^{-1}$]
Ω
0.0
0.2
0.4
0.6
0.8
1.0

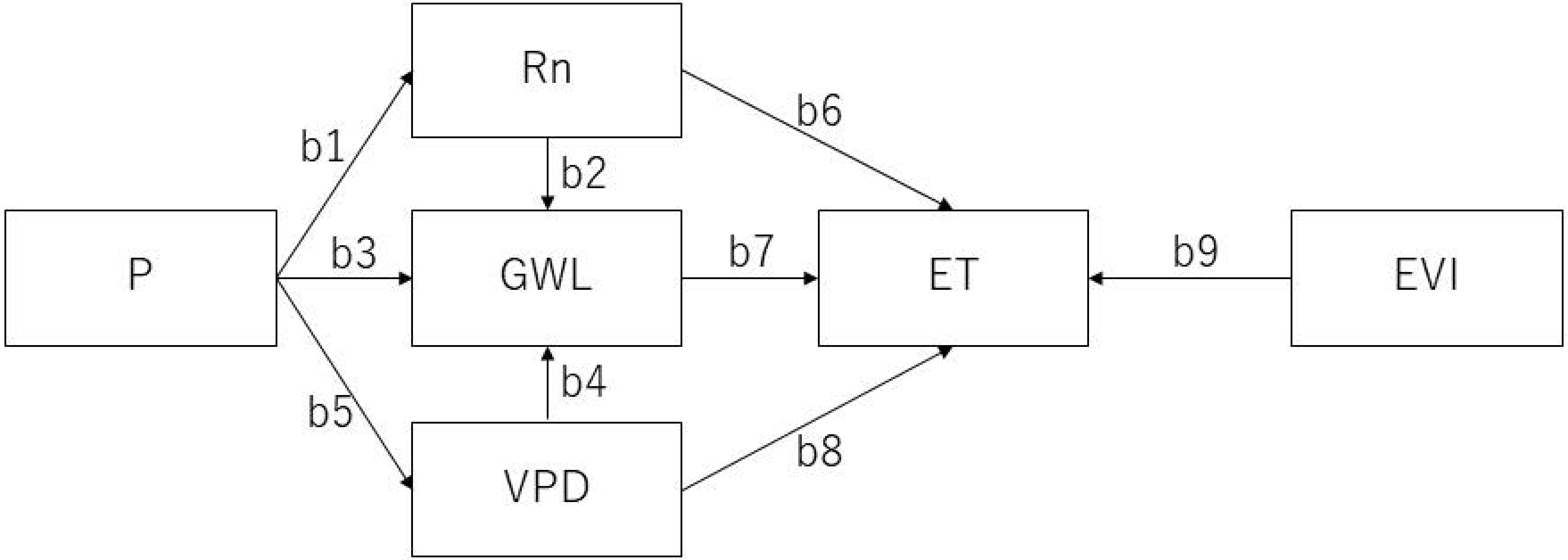
Rn
b1
b2
b6
P
b3
GWL
b7
ET
b9
EVI
b4
b5
b8
VPD

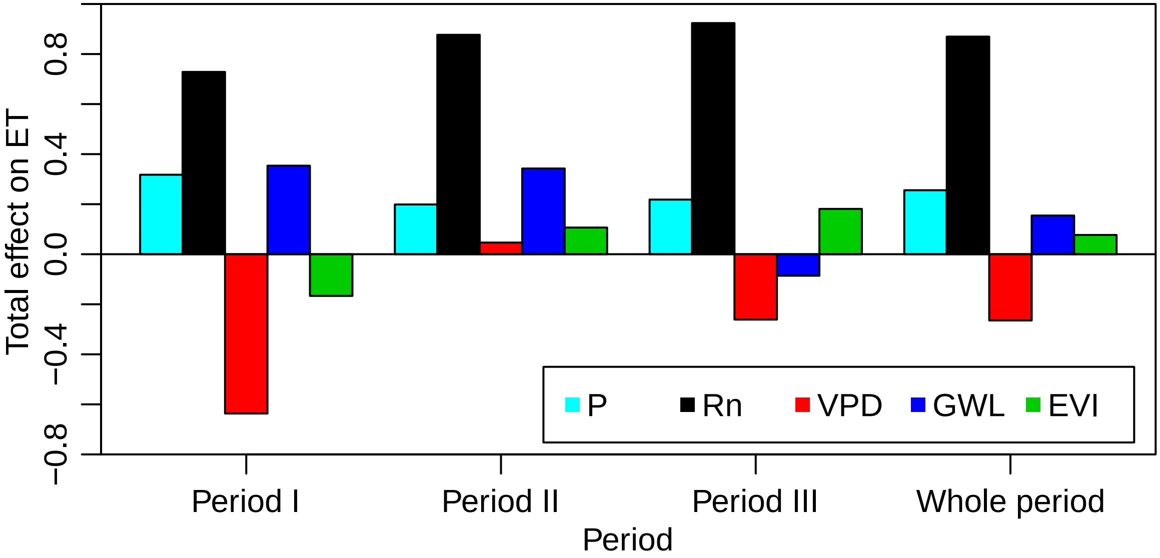
Total effect on ET
0.8
0.4
0.0
−0.4
−0.8
P
Rn
VPD
GWL
EVI
Period I
Period II
Period III
Whole period
Period